Reprinted from
Volume 281, Number 11 **March 17, 2006**

The Journal of Biological Chemistry

WARP Is a Novel Multimeric Component of the Chondrocyte Pericellular Matrix That Interacts with Perlecan

Justin M. Allen, John F. Bateman, Uwe Hansen, Richard Wilson, Peter Bruckner, Rick T. Owens, Takako Sasaki, Rupert Timpl, and Jamie Fitzgerald

American Society for Biochemistry and Molecular Biology

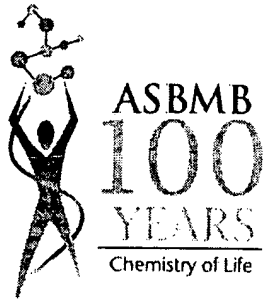

THE JOURNAL OF BIOLOGICAL CHEMISTRY VOL. 281, NO. 11, pp. 7341–7349, March 17, 2006

WARP Is a Novel Multimeric Component of the Chondrocyte Pericellular Matrix That Interacts with Perlecan*

Received for publication, December 27, 2005 Published, JBC Papers in Press, January 6, 2006, DOI 10.1074/jbc.M513746200

Justin M. Allen[‡1], John F. Bateman[‡], Uwe Hansen[§], Richard Wilson[‡], Peter Bruckner[§], Rick T. Owens[¶], Takako Sasaki[‖], Rupert Timpl[‖†], and Jamie Fitzgerald[‡2]

From the [‡]Cell and Matrix Biology Research Unit, Murdoch Childrens Research Institute and Department of Paediatrics, University of Melbourne, Royal Children's Hospital, Parkville, Victoria 3052, Australia, [§]Institute for Physiological Chemistry and Pathobiochemistry, University Hospital of Muenster, 48129 Muenster, Germany, [¶]LifeCell Corporation, Branchburg, New Jersey 08876, and [‖]Max-Planck-Institute for Biochemistry, D-82152 Martinsried, Germany

WARP is a novel member of the von Willebrand factor A domain superfamily of extracellular matrix proteins that is expressed by chondrocytes. WARP is restricted to the presumptive articular cartilage zone prior to joint cavitation and to the articular cartilage and fibrocartilaginous elements in the joint, spine, and sternum during mouse embryonic development. In mature articular cartilage, WARP is highly specific for the chondrocyte pericellular microenvironment and co-localizes with perlecan, a prominent component of the chondrocyte pericellular region. WARP is present in the guanidine-soluble fraction of cartilage matrix extracts as a disulfide-bonded multimer, indicating that WARP is a strongly interacting component of the cartilage matrix. To investigate how WARP is integrated with the pericellular environment, we studied WARP binding to mouse perlecan using solid phase and surface plasmon resonance analysis. WARP interacts with domain III-2 of the perlecan core protein and the heparan sulfate chains of the perlecan domain I with K_D values in the low nanomolar range. We conclude that WARP forms macromolecular structures that interact with perlecan to contribute to the assembly and/or maintenance of "permanent" cartilage structures during development and in mature cartilages.

The extracellular matrix (ECM)[3] is a complex and dynamic three-dimensional environment that plays fundamental roles in morphogenesis and development, tissue structure, repair, and metastasis (1). The tissue-specific expression of collagen types and specialized ECM components results in the formation of architecturally precise interacting networks with unique functional and biological characteristics. A diverse range of ECM components have been described including more than 20 distinct collagen subtypes and a large number of proteoglycans and noncollagenous proteins. Many of these matrix proteins are modular in structure in that they are composed of protein domains, which is important in generating the multifunctionality that is characteristic of ECM proteins (2, 3). One of these domains, found in a growing number of ECM proteins involved in supramolecular structures, is the A domain first described in von Willebrand factor (VWA domain). VWA domains are found in a diverse range of ECM proteins including collagens (types VI, VII, XII, XIV, XX, XXI, XXVII, and XXVIII), matrilins, cochlin, polydom, AMACO (VWA-like domains related to those in matrilins and collagens), and the extracellular portions of nine transmembrane α-integrin chains (4–6)

We recently identified a new member of the von Willebrand factor A domain superfamily, WARP (von Willebrand factor A domain-related protein), that may have evolved from a collagen-like molecule (7, 8). The WARP protein comprises a single N-terminal VWA domain containing a putative metal ion-dependent adhesion site motif, two fibronectin type III repeats, and a unique C-terminal segment. Our studies demonstrated WARP expression by chondrocytes, and in transfected cells WARP is a secreted glycoprotein that can form multimeric structures (7). We report here that in mouse cartilage WARP defines the presumptive articular cartilage prior to joint cavitation and subsequently during development is present in articular cartilage as well as in several fibrocartilage elements. Biochemical analysis demonstrated that WARP exists as disulfide-bonded multimers in cartilage tissue. Furthermore, we show that WARP can strongly interact with perlecan, providing a mechanism by which WARP is integrated into the extracellular matrix of cartilage.

EXPERIMENTAL PROCEDURES

cDNA Constructs and Cell Culture—The hexahistidine-tagged WARP constructs in the pCEP4 vector (7) containing single Cys-to-Ser mutations at amino acid 369 or 393 and the double mutant (C369S/C393S) were generated by strand overlap extension PCR (9). The wild-type and mutant His-WARP cDNAs were transfected into HEK 293-EBNA cells using FuGENE 6 transfection reagent (Roche Applied Science) and grown as described (7).

WARP Immunoprecipitations—Transfected cells were grown to confluence in 35-mm dishes and labeled for 18 h with 300 μCi of L-[^{35}S]methionine (1388 Ci/mmol; PerkinElmer Life Sciences) in Dulbecco's modified Eagle's medium as described previously (7). Briefly, the cell and medium fractions were collected in the presence of protease inhibitors, and His-tagged WARP was immunoprecipitated from the cell and medium fractions with anti-His antibody (Roche Applied Science) (0.5 μg/ml) and protein A-Sepharose overnight. Following washing, the immunoprecipitated material was denatured and fractionated on a 7.5% (v/v) SDS-polyacrylamide gel and subjected to fluorography.

* This work was supported by National Health and Medical Research Council of Australia Grant 284524 (to J. F. and J. F. B.), a grant from the Murdoch Childrens Research Institute (to J. F.), and Deutsche Forschungsgemeinschaft Sonderforschungsbereich 492, A2. The costs of publication of this article were defrayed in part by the payment of page charges. This article must therefore be hereby marked "*advertisement*" in accordance with 18 U.S.C. Section 1734 solely to indicate this fact.

† Deceased October, 2003.

[1] Supported by an Australian Postgraduate Award Scholarship and the Murdoch Childrens Research Institute.

[2] To whom correspondence should be addressed: Cell and Matrix Biology, Murdoch Childrens Research Institute, Royal Children's Hospital, Flemington Rd., Parkville, Victoria 3052, Australia. Tel.: 61-3-9345-6263; Fax: 61-3-9345-7997; E-mail: j.fitzgerald@mcri.edu.au.

[3] The abbreviations used are: ECM, extracellular matrix; VWA, von Willebrand factor A; GAG, glycosaminoglycan; CHAPS, 3-[(3-cholamidopropyl)dimethylammonio]-1-propanesulfonic acid; GST, glutathione *S*-transferase; BSA, bovine serum albumin; PBS, phosphate-buffered saline; En, embryonic day *n*; FGF, fibroblast growth factor.

Cartilage Sample Preparation—Femoro-tibial joint and rib cartilage was dissected from newborn mice and powdered in a liquid nitrogen-cooled Spex freezer mill and dissolved in neutral salt buffer (40 mM Tris-HCl, pH 7.5, 10 mM EDTA containing Complete protease inhibitor mixture; Roche Applied Science). Following sonication, the soluble material was collected (fraction 1), and the insoluble material was treated overnight at 37 °C with 0.02 units of chondroitinase ABC (Seikagaku) and 1 unit of hyaluronidase (Sigma) to cleave hyaluronan and chondroitin sulfate GAG chains. Following washing the soluble material was collected (fraction 2), and the insoluble pellet was dissolved in 6 M GuHCl, 40 mM Tris-HCl, pH 7.5, 10 mM EDTA containing protease inhibitors for 5 h at 4 °C and then centrifuged at room temperature for 20 min. The supernatant was saved as soluble fraction 3, the matrix components were precipitated with 95% ethanol, and the pellet was washed with 70% ethanol. The samples were then freeze-dried and resuspended in 200 μl of 8 M urea, 4% CHAPS, 40 mM Tris base, and 2 mM tributyl phosphine (Bio-Rad). For some experiments the reducing agent tributyl phosphine was omitted.

Antibodies—Polyclonal antisera against the VWA domain and C-terminal domains of WARP were produced commercially in rabbits (Institute of Medical and Veterinary Science, Adelaide, Australia) using the GST-VWA domain (amino acids 21–212) and the maltose-binding protein-C-terminal domain (amino acids 389–415) fusion proteins expressed in bacteria as antigens. The antisera bound to the fusion proteins in a dose-dependent manner in a standard enzyme-linked immunosorbent assay (not shown). The anti-VWA domain WARP polyclonal antibody was further affinity-purified against the antigen immobilized on a nitrocellulose membrane as described elsewhere (10) and used in immunohistochemical staining experiments at a final concentration of 1 μg/ml. Briefly, the GST-VWA domain fusion protein was transferred to nitrocellulose following SDS-PAGE. The band was visualized by staining with 0.1% Ponceau S (w/v) in 5% acetic acid and cut out. The nitrocellulose strip was destained, blocked with 3% BSA in PBS, and incubated with the anti-VWA antiserum overnight at 4 °C. Following washing, bound antibody was eluted with 0.1 M glycine-HCl, pH 2.5, neutralized by the addition of 1 M Tris-HCl, pH 8.0. The polyclonal anti-C-terminal antiserum was used at a dilution of 1:1000 in immunohistochemistry and immunoblots and 1:200 in solid phase assays. Serum from the same rabbit, taken prior to immunization with the WARP fusion protein, was used as a negative control. For immunogold electron microscopy experiments, a polyclonal antibody raised in sheep against full-length recombinant WARP (described under "Recombinant Proteins") was used.

An antibody to bovine matrilin-1 was kindly provided by Prof. Mats Paulsson (University of Cologne, Cologne, Germany) and was used at a dilution of 1:3000 for immunohistochemistry or 1:500 for immunoblotting. Affinity-purified antibody against mouse perlecan domain V (11) was used at a final concentration of 2 μg/ml in immunohistochemical experiments. A monoclonal antibody against perlecan (MAB 1948; Chemicon), was used in the immunogold experiments.

WARP Immunoblotting—Fractions 1, 2, and 3 (20 μg) were denatured by heating at 95 °C for 5 min, separated on a 10% polyacrylamide gel, and transferred to Immobilon™-P polyvinylidene difluoride membrane (Millipore). The membrane was blocked in 5% milk powder in PBS for 1 h and then incubated in antibody buffer (0.5% milk powder in PBS with 0.1% Tween 20) containing either WARP (1:1000 dilution) or matrilin-1 antisera for 1 h. Following three washes in PBS with 0.1% Tween 20, anti-rabbit IgG horseradish peroxidase secondary antibody (Dako) was added at a dilution of 1:10,000 in antibody buffer and incubated for 1 h. Following washing, the signal was developed with ECL Plus Western blotting detection system (Amersham Biosciences) and autoradiography using X-Omat film.

WARP Immunohistochemistry—Embryonic mouse tissues were surgically removed and frozen in Tissue-Tek O.C.T. compound (Circle Scientific). Tissues from post-natal mice were fixed in Histochoice (Amresco) overnight at 4 °C before decalcification in PBS with 7% (w/v) EDTA. 10-μm sections were mounted and fixed in 95% ethanol, 5% acetic acid or in Histochoice (Amresco). To facilitate antibody penetration into the ECM, sections were treated with 0.2% hyaluronidase (bovine, type IV; Sigma) and treated with 0.3% H_2O_2 (v/v) in methanol to inactivate endogenous peroxidases. After blocking with 1% BSA (w/v) in PBS, the sections were immunolabeled with the rabbit antisera or preimmune serum and detected using the Vectastain Elite ABC kit (Vector Laboratories). Bound antibodies were visualized using Sigma-Fast DAB tablets, and sections were counterstained with hematoxylin.

For immunogold electron microscopy, native suprastructural fragments were isolated from human articular cartilage and placed on grids. Samples were doubly immunostained with polyclonal sheep antisera against full-length WARP (or the VWA domain or C-terminal WARP, described above) and a monoclonal antibody against perlecan and colloidal gold-labeled secondary antibodies of different sizes and analyzed with transmission electron microscopy as described (12).

In Situ Hybridization—15-μm cryosections were fixed with 4% paraformaldehyde in PBS for 15 min. Nonspecific probe binding was blocked by carbethoxylation with 0.1% active diethyl pyrocarbonate in PBS twice for 15 min before prehybridization in buffer containing 50% formamide, 5× SSC, and 40 μg/ml salmon sperm for 2 h at 58 °C. Hybridization solution was prepared by adding a 1-kb digoxigenin-labeled riboprobe complementary to the 3′-untranslated region of WARP, or the sense orientation negative control, to prehybridization solution at 400 ng/ml and denatured at 80 °C. The sections were hybridized at 58 °C overnight and washed with 2× SSC and 1× SSC for 1 h at 65 °C. Immunodetection was performed as described elsewhere (13).

Recombinant Proteins—Recombinant His-WARP was purified from the media of transfected 293-EBNA cells using nickel ion affinity chromatography as described for decorin (14). Fractions enriched for WARP dimer were used for subsequent interaction analyses (see Fig. 5).

Recombinant mouse perlecan domain IA containing heparan sulfate (15); mutant domain I lacking heparan sulfate (16); domains II (17); subdomains III-1, III-2, and III-3 (18); subdomains IV-1 and IV-2 (19); and domain V (11) were expressed in 293-EBNA cells and purified as described. Protein concentrations were determined by amino acid analysis. Full-length perlecan was purified from mouse Engelbreth-Holm-Swarm tumor (20).

Solid Phase Binding Assay—Multiwell plates (96 wells, Immulon 4; Dynatech) were coated with recombinant proteins (1 or 5 μg/ml, 50 μl/well) or heparin (1 μg/ml) (Sigma) isolated from porcine intestinal mucosa in enzyme-linked immunosorbent assay coating buffer (50 mM sodium carbonate, pH 9.2) overnight at room temperature. Following four wash buffer (0.15 M NaCl, 0.05% Tween 20) rinses, nonspecific binding sites were blocked for 1 h with Tris-buffered saline (0.15 M NaCl, 50 mM Tris, pH 7.4) containing 1% BSA. Incubations with recombinant WARP (0–200 nM) were carried out in Tris-buffered saline for 1 h. In some experiments 5 mM $CaCl_2$ or 10 mM EDTA was included in WARP incubations and the subsequent washes. Incubation with the primary polyclonal antibodies (diluted 1:200) against the soluble ligands was followed by incubation with anti-rabbit IgG horseradish peroxidase-conjugated secondary antibody (diluted 1:1000; Dako). Color was developed with 2,2′-azino-bis(3-ethylbenzthiazoline-6-sulfonic acid (ABTS) in citrate buffer (0.1% (w/v) ABTS, 0.03% H_2O_2, 61 mM citrate,

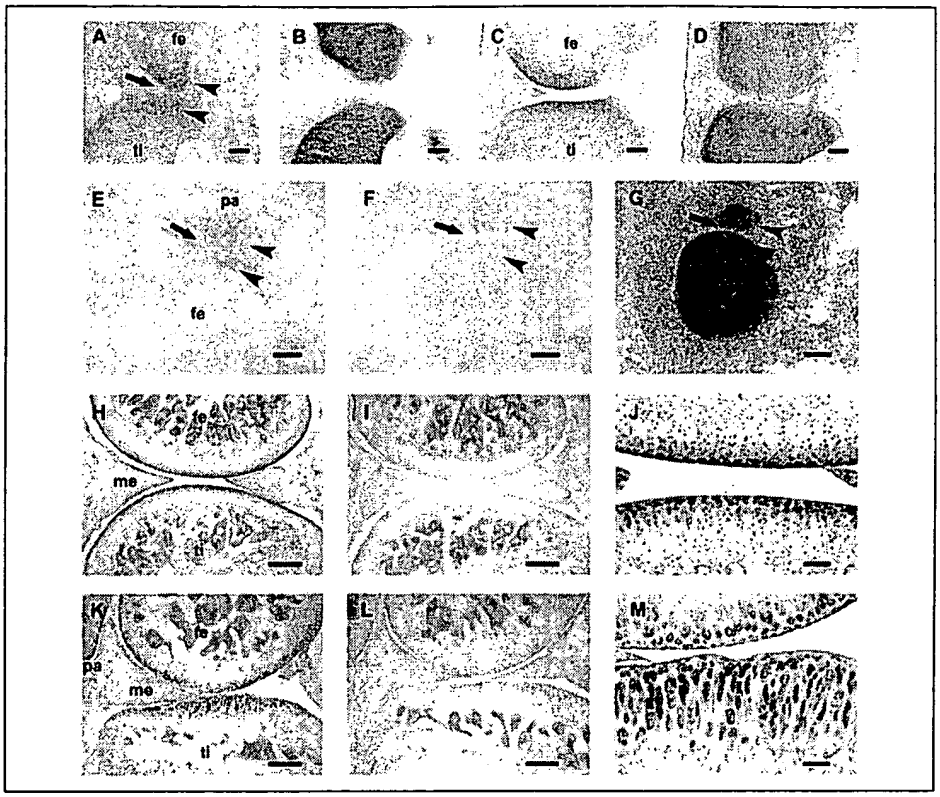

FIGURE 1. **Distribution of WARP mRNA and protein in developing articular cartilage.** WARP protein was restricted to the chondrogenous layers (*arrowheads*), but not the intermediate layer (*arrow*), of the joint interzone at E15.5 (*A*) and to the presumptive articular cartilage at E18.5 (*C*). Matrilin-1 was absent from the developing articular cartilage but was detected throughout the underlying epiphyseal cartilage (*B* and *D*). WARP mRNA was expressed by cells of the chondrogenous zone of the interzone (*arrowheads*) between the femur and patella at E14.5 (*E*) in a frontal section of the knee joint but was absent from the intermediate layer (*arrow*) and the epiphyseal cartilage. No hybridization with the sense probe was detected (*F*). Histology was performed with Alcian Blue, hematoxylin, and eosin (*G*). In the 2-week-old knee joint, WARP immunostaining was pericellular throughout the superficial zone of the femoral and tibial articular cartilage and in the meniscus (*H* and *J*). In addition to these sites, in 6-week-old mice WARP was detected through the intermediate zones of the femoral and tibial articular cartilage and the superficial zone of the patella (*K* and *M*). Control sections from 2-week-old (*I*) and 6-week-old (*L*) mice were probed with WARP preimmune serum. The *scale bars* are 100 μm (*A–G*), 250 μm (*H, I, K,* and *L*), and 50 μm (*J* and *M*). *fe*, femur; *ti*, tibia; *pa*, patella; *me*, meniscus.

77 mM $Na_2HPO_4.2H_2O$ pH 4.0), and color yields were determined at 405 nm using a microtitre plate reader (model 450; Bio-Rad). Nonspecific binding to 1% BSA was subtracted from each absorbance reading.

Surface Plasmon Resonance Analysis—The BIAcore 3000 system (BIAcore AB) was used to characterize interactions between WARP and perlecan and WARP self-association. Purified recombinant proteins were immobilized to a CM5 sensor chip at 25 °C at a flow rate of 5 μl/min. The sensor chip was activated with a 35-μl mixture of 50 mM *N*-hydroxysuccinimide and 200 mM *N*-ethyl-*N'*-(dimethylaminopropyl) carbodiimide. WARP (30 μg/ml) in 5 mM sodium malate, pH 6.0, or perlecan subdomain III-2 (30 μg/ml) in sodium citrate, pH 3.35, were coupled. The remaining active groups were blocked with 1 M ethanolamine HCl, pH 8.5. A control surface containing no immobilized ligand was prepared by activation and blocking in the absence of ligand. The immobilization resulted in 3500–4200 resonance units for WARP and 3600 resonance units for perlecan subdomain III-2. Binding studies were performed in HEPES-buffered saline buffer (10 mM HEPES, pH 7.4, 0.15 M NaCl, 5 mM $CaCl_2$, 0.005% P-20) at a flow rate of 5 μl/min, and the binding sites of the immobilized ligands were regenerated using a 12-s pulse of either 30 or 50 mM NaOH at 50 μl/min. WARP was immobilized (3900 response units) to the C1 biosensor surface in 10 mM sodium acetate, pH 5.0. The perlecan domain 1 binding studies were performed as described above except that WARP surface was regenerated using a 6s pulse of 10 mM NaOH and the experiment was carried out at a flow rate of 30 μl/min. For the kinetic analyses, the flow rates were performed at 30 μl/min. In one experiment WARP was coupled directly to the sensor chip (990 response units). Alternatively WARP (30 μg/ml, 5-min injection) was bound to immobilized anti-His antibody (9000 response units). After subtraction of blank curves, the association (k_a) and dissociation (k_d) rate constants were determined simultaneously using global curve fits to the equation for 1:1 Langmuir binding in the BIAevaluation 3.2 software (BIAcore AB).

RESULTS

Distinct Localization of WARP in Joint Cartilage during Development—The spatial distribution of WARP in the developing mouse knee joint was assessed during development at E15.5 and E18.5 and later in the 2- and 6-week-old knee joint. Immunohistochemistry was performed using the polyclonal antibody raised to the WARP C-terminal domain, with the corresponding preimmune serum used as a negative control. The results were verified by immunostaining with the WARP anti-VWA domain antibody (data not shown).

At E15.5, the joint cavity between the cartilage rudiments of the femur and tibia had not formed. The femur and tibia anlagen were separated by the joint interzone, consisting of two chondrogenous layers separated by an intermediate zone of mesenchymal cells, which will differentiate to form the articular surfaces and the joint cavity. At E15.5 WARP was present in the chondrogenous layers of the joint interzone of the femur and tibia (Fig. 1*A*) but was absent from the underlying epiphyseal cartilage and the noncartilaginous intermediate layer of the future joint space. In comparison, antibodies against another VWA domain superfamily member used as a marker for developing cartilaginous structures, matrilin-1, strongly labeled the cartilage anlage of the developing femur and tibia but not the joint interzone (Fig. 1*B*). In E18.5 mice, WARP protein was restricted to ~6–10 cell layers extending from the articular surface (Fig. 1*C*). Matrilin-1 was absent from this developing articular zone but was abundant throughout the epiphyses of the femur and tibia (Fig. 1*D*). No staining was detected with the preimmune serum (not shown).

To determine the site of WARP mRNA expression during early joint development, *in situ* hybridization was performed on frontal sections from an E14.5 mouse knee joint. Consistent with the distribution of WARP protein, WARP mRNA was expressed by cells of the two chondrogenous layers of the joint interzone separating the femur and patella

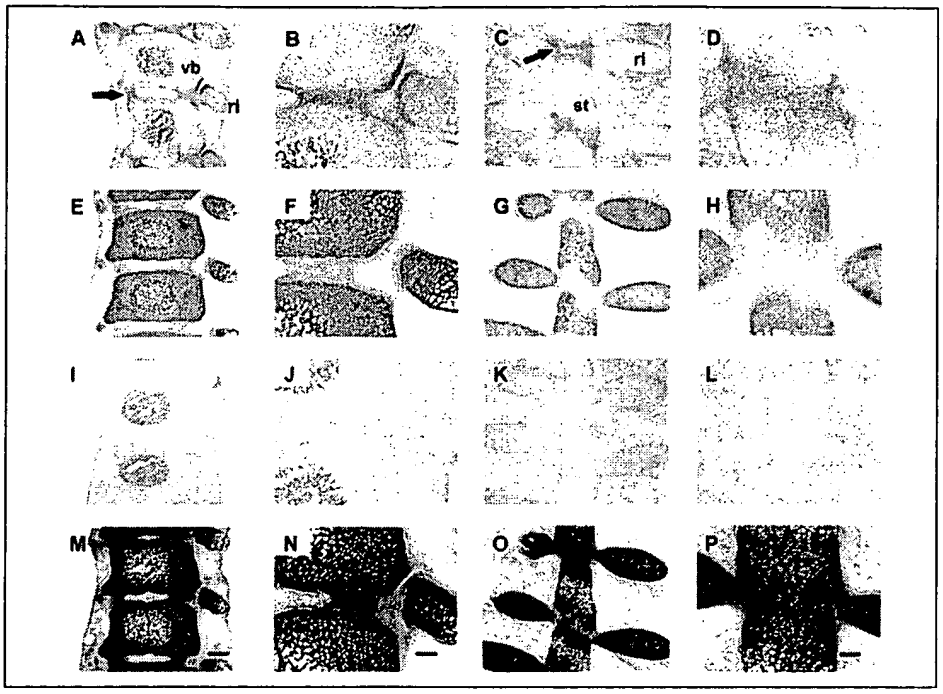

FIGURE 2. **Immunohistochemical detection of WARP and matrilin-1 in E18.5 spine and sternum.** In spine, WARP protein had a pericellular distribution throughout the annulus fibrosus (*arrow*) of the intervertebral disc and the articular surfaces of the rib and vertebrae (*A* and *B*). Matrilin-1 was barely detectable in these structures but was abundant throughout the cartilage anlage of the developing vertebral bodies and ribs (*E* and *F*). In the sternum, WARP protein was restricted to the synarthrodial joints (*arrow*) between the sternebrae (*C* and *D*). Matrilin-1 antibodies strongly immunolabeled the cartilage anlage of the ribs and sternebrae but was absent from the synarthrodial joints (*G* and *H*). Control sections were probed with WARP preimmune serum (*I–L*). Cartilage proteoglycans were visualized with Toluidine Blue O, and the sections were counterstained with Fast Green FCF (*M–P*). For each spine and sternum set of images the *scale bars* of the panels on the *left* are 250 μm, and those of the panels on the *right* are 100 μm. *vb*, vertebral bodies; *ri*, rib; *st*, sternebrae.

but was absent from the mesenchymal intermediate layer of the interzone and from the epiphyseal cartilage (Fig. 1*E*). No signal was seen with the sense orientation negative control (Fig. 1*F*).

In 2-week-old mice, after development of the secondary ossification center, WARP localized to the pericellular matrix primarily around superficial zone chondrocytes of the femoral and tibial articular cartilage (Fig. 1, *H* and *J*) and could also be detected in the superficial layers of the meniscus (Fig. 1*H*) and the patella (not shown). In 6-week-old articular cartilage, the distribution of WARP was clearly restricted to the pericellular matrix, with no detectable interterritorial matrix staining (Fig. 1, *K* and *M*). Pericellular WARP immunolabeling was also seen in the meniscus, the patella, and the intermediate as well as superficial zones of the femoral and tibial articular cartilage. No immunostaining was detected in sections probed with the preimmune serum (Fig. 1, *I* and *L*).

WARP Also Localizes to the Permanent Cartilages of Spine and Sternum—In the spine, immunostaining for WARP was restricted to the articular surfaces of the ribs and vertebrae at the costo-vertebral joint and barely detectable in the rib costal cartilage and vertebral body (Fig. 2*A*). WARP also exhibited a pericellular staining pattern throughout the annulus fibrosus of the intervertebral disc (Fig. 2*B*). In contrast, matrilin-1 antibodies strongly labeled the cartilage anlage of the developing vertebral bodies and ribs (Fig. 2, *E* and *F*) and was barely detectable in articular cartilage of the costo-vertebral joint and in the annulus fibrosus, in a distribution complementary to that of WARP.

In the embryonic sternum, WARP exhibits a pericellular distribution in the fibrocartilaginous synarthrodial joint between each sternebrae (Fig. 2, *C* and *D*) and is absent from the anlage of the developing ribs and sternebrae. Strong matrilin-1 immunoreactivity was detected throughout the embryonic anlage of the ribs and sternebrae but was absent from the synarthrodial joint (Fig. 2, *G* and *H*). This distribution is complementary to that of WARP, a consistent observation from analysis of the developing joint and spine.

WARP Forms Disulfide-bonded Multimers in Cartilage—To assess whether WARP forms multimeric structures *in vivo*, mouse cartilage preparations were serially extracted under progressively more denaturing conditions and the solubilized material in each extract subjected to immunoblot analysis using WARP antisera. Serial extraction of femorotibial joint cartilage, first with neutral salt buffer and then extraction of the insoluble material with hyaluronidase and chondroitinase ABC to degrade hyaluronan and chondroitin sulfate GAG chains and release interacting proteins, did not extract WARP (Fig. 3*A*, *lanes 1* and *2*). However, extraction of the remaining insoluble material with the strong denaturant 6 M guanidine HCl solubilized WARP protein, which was detected as a band on SDS-polyacrylamide gels migrating at ~50 kDa when resolved under reducing conditions (*lane 3*), consistent with the predicted molecular mass of the WARP monomer (7). The ECM "adaptor" molecule, matrilin-1, was also present in the guanidine-soluble extract (*lane 4*), in agreement with published data (21). The finding that WARP is solubilized by 6 M guanidine HCl suggests that, as with matrilin-1, WARP is a strongly interacting component of the cartilage ECM. When resolved without reduction, WARP migrated as disulfide-bonded oligomeric forms greater than 200 kDa (Fig. 3*B*, *lane 1*). Immunoblot analysis on conditioned media from cells transfected with WARP cDNA confirms that WARP assumes several multimeric forms, including a dimer at 100 kDa, that are reducible to a 50-kDa monomer (Fig. 3*B*, *lanes 2–4*). These multimers were also formed by purified recombinant WARP, confirming that these structures are likely to be oligomers of WARP rather than WARP bound to other molecules (*lanes 5* and *6*).

The ability of WARP to self-associate was assessed in BIAcore biosensor experiments where WARP coupled to the sensor chip surface was challenged with WARP in solution (Fig. 3*C*). Soluble WARP (120–720 nM) bound to immobilized WARP in a dose-dependent manner. Global or local curve fitting using BIA evaluation software (v3.2) failed to fit these binding curves using the Langmuir 1:1 model, suggesting that the WARP-WARP interactions reflect complex self-associations, consistent with WARP multimerization.

To test whether one or both Cys residues are involved in multimer stabilization, the two C-terminal cysteines were mutated to serine residues separately and in tandem (Fig. 3*D*), and their effects on multimerization were assessed in transfected cells (Fig. 3*E*). Because the majority of WARP is present in the medium fraction rather than the cell

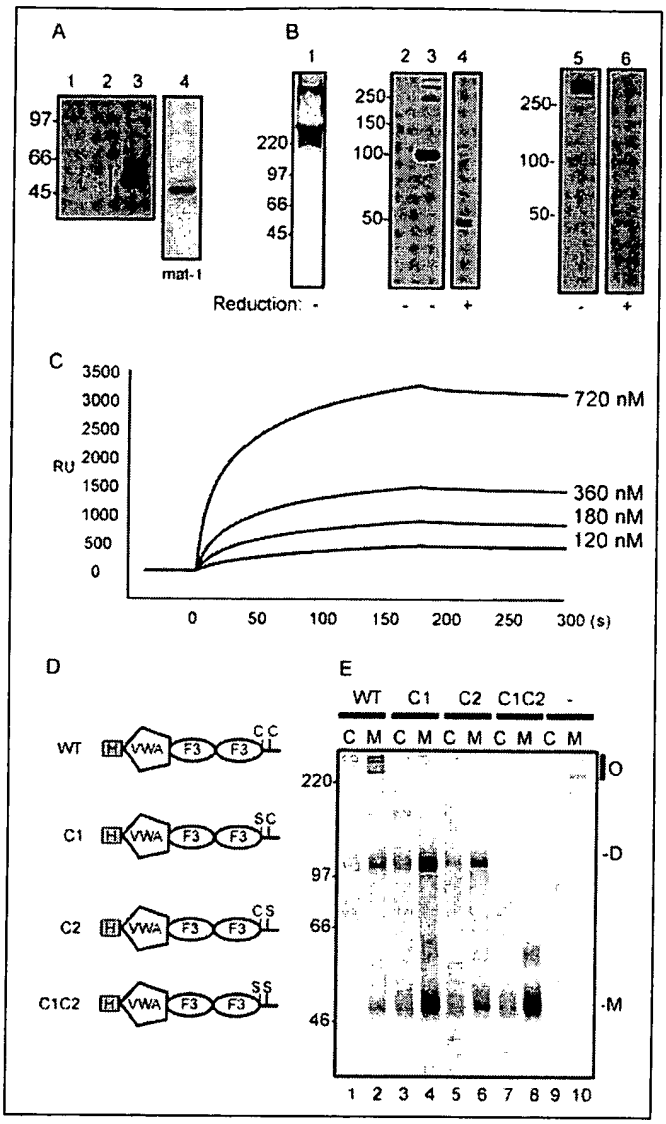

FIGURE 3. **Analysis of WARP multimers.** *A*, serial extraction of WARP from cartilage. 20 μg of protein solubilized in neutral salt buffer (*lane 1*), following hyaluronidase/chondroitinase ABC digestion (*lane 2*), and 6 M guanidine HCl extraction (*lanes 3* and *4*) was resolved under reducing conditions on 10% (v/v) polyacrylamide gels and immunoblotted using either WARP anti-VWA (*lanes 1–3*) or matrilin-1 (*lane 4*) polyclonal antisera. Migration positions of molecular mass markers (kDa) are indicated on the *left*. *B*, multimerization of WARP. Guanidine HCl extracts (20 μg) of cartilage isolated from rib (*lane 1*) were analyzed by immunoblotting after electrophoresis under nonreducing conditions. Conditioned media from 293-EBNA cells transfected with WARP cDNA (*lanes 3* and *4*) were resolved without (*lanes 2* and *3*) and with reduction (*lane 4*) and analyzed by immunoblotting. Lack of bands in untransfected cells (*lane 2*) demonstrates specificity of the WARP antisera. Purified His-tagged recombinant WARP was also analyzed by SDS-PAGE in the absence (*lane 5*) or presence of reducing agents (*lane 6*). WARP was detected by immunoblotting with the anti-VWA domain antibody (*lane 1*) or the anti-C-terminal domain antibody (*lanes 2–4*), or by silver staining (*lanes 5* and *6*). *C*, analysis of WARP multimerization by surface plasmon resonance. WARP immobilized on a CM5 sensor chip was presented with WARP dimer in solution (0.72, 0.36, 0.18, and 0.12 μM) injected at a flow rate of 5 μl/min. *D*, diagram of WARP cysteine mutants. The domain structure of WARP comprises an N-terminal VWA domain and two fibronectin type III repeats (*F3*) followed by a short C-terminal domain. Cysteine-to-serine single and double point mutations were introduced at Cys^{369} and Cys^{393}. *E*, analysis of WARP multimerization *in vitro*. 293-EBNA cells expressing wild type (*WT*, *lanes 1* and *2*), C369S (C1) (*lanes 3* and *4*), C393S (C2) (*lanes 5* and *6*), C369S/C393S (C1C2) His-WARP mutant (*lanes 7* and *8*), and untransfected cells (*lanes 9* and *10*) were metabolically labeled for 16 h with [^{35}S]methionine and His-WARP immunoprecipitated from media (*lanes M*) and cell lysates (*lanes C*) using an anti-His antibody. The samples were resolved by 7.5% (v/v) SDS-polyacrylamide gel under nonreducing conditions, and the radiolabeled proteins were visualized by fluorography. The migration positions of monomers (*M*), dimers (*D*), and oligomeric structures (*O*) are noted on the *right*, and molecular mass markers are on the *left* (kDa). *RU*, response unit(s).

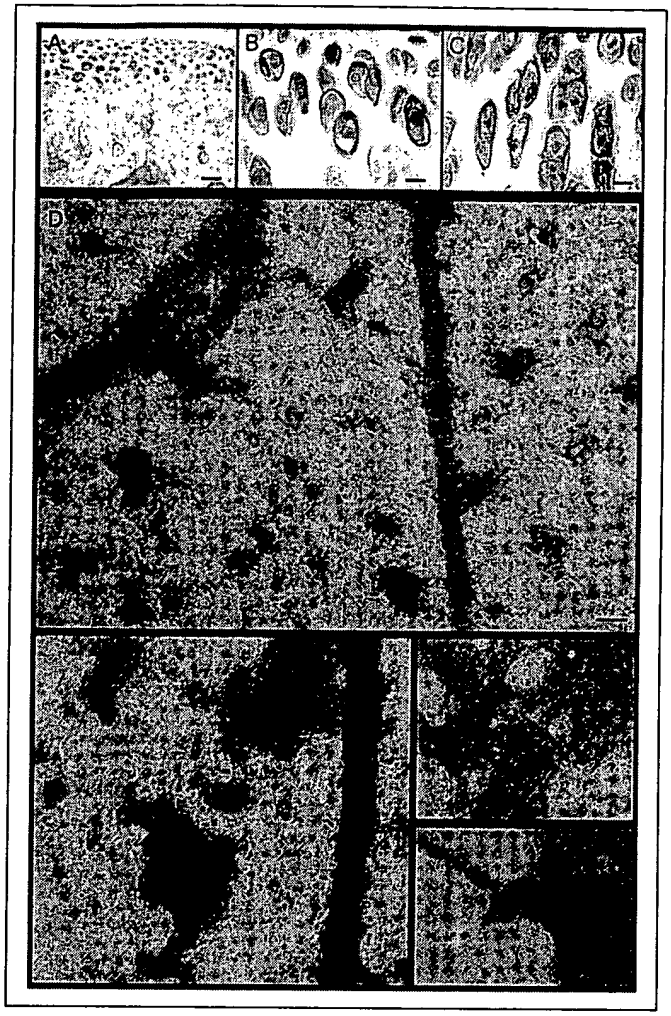

FIGURE 4. **WARP and perlecan co-localize in articular cartilage.** Perlecan localizes to the articular cartilage of 6-week-old mice (*A*). Higher magnification of articular cartilage in *A* is shown in *B*. Note the perlecan staining in the pericellular microenvironment. For comparison, the pericellular localization of WARP is shown in *C*. Representative micrographs showing the co-localization of WARP and perlecan in native fibrils extracted from human articular cartilage visualized by electron microscopy (*D*). Immunogold particles (WARP, 18-nm particles; perlecan, 12-nm particles) were localized within the extrafibrillar material in close association. The *scale bars* are 50 μm in *A*, 10 μm in *B* and *C*, and 100 nm in *D*.

fraction of all four transfected cell lines, the introduced mutations did not result in intracellular accumulation of the mutant protein. In cells expressing the wild-type chain, WARP migrated primarily as dimeric and higher order forms with several discrete bands greater than 250 kDa (*lane 2*) that were identified as WARP in immunoblotting experiments (Fig. 3*B*). The C1 and C2 single cysteine mutants both migrated as a monomer and a dimer with no higher molecular mass structures evident (*lanes 3–6*). As expected, disulfide-bonded dimers or multimers were not detected in the C1C2 double mutant, which migrated only as a monomer (*lanes 7* and *8*). These data suggest that both Cys residues can participate in disulfide bond formation and that both Cys residues are required to stabilize the higher molecular mass WARP oligomers.

WARP Co-localizes with Perlecan—Our finding that WARP forms multimeric structures in the cartilage extracellular environment raises the possibility that, like other multimeric components such as matrilins, WARP interacts with different cartilage ECM molecules. Because it has been reported that perlecan, a large multidomain proteoglycan that is essential for skeletal development, is a component of the cartilage peri-

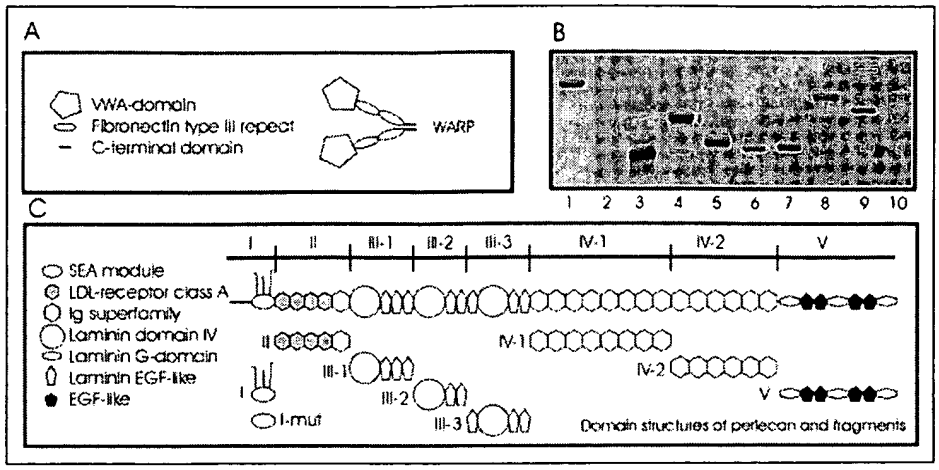

FIGURE 5. **Modular structure of WARP, perlecan, and perlecan fragments.** Shown are diagrams of WARP (*A*) and perlecan fragments (*C*) and protein samples used in interaction analysis (*B*). Recombinant protein samples were resolved on 10% (v/v) SDS-polyacrylamide gel, and the gel was subjected to silver staining. The samples are: WARP (*lane 1*); perlecan domain I (*lane 2*); domain I-mut lacking heparan sulfate GAG chains (*lane 3*); domain II (*lane 4*); subdomains III-1, -2, and -3 (*lanes 5–7*); subdomains IV-1 and -2 (*lanes 8* and *9*); and domain V (*lane 10*). Note that the heparan sulfate GAG chains present on domain I prevents the core protein from taking up the silver stain. Diagram of modular structure of perlecan shown in *C* is adapted from Ref. 35.

cellular environment (22–26), we assessed whether WARP and perlecan co-localize in articular cartilage. We performed immunohistochemistry on mouse articular cartilage from 6-week-old mice and immunogold electron microscopy on human articular cartilage extract using antisera against WARP and monoclonal antibodies against perlecan (Fig. 4). In 6-week-old mice perlecan was present in articular cartilage and specifically localized to the chondrocyte pericellular region (Fig. 4, *A* and *B*) in a pattern that was strikingly similar to that of WARP (Figs. 1*M* and 4*C*).

Immunogold electron microscopy was performed on extracts of human articular cartilage using an antibody against recombinant full-length WARP (18-nm particles) and a monoclonal anti-perlecan antibody (12-nm particles) (Fig. 4*D*). Both molecules were frequently found in close association within the amorphous extrafibrillar material, providing further evidence that WARP and perlecan co-localize in articular cartilage. The immunogold EM experiments were repeated using the VWA domain and C-terminal WARP antisera, and the same pattern of co-localization with perlecan was demonstrated (data not shown).

WARP Interacts with Perlecan—We have established that WARP is a multimeric ECM component that localizes to the same connective tissue compartment as perlecan in cartilage. To investigate whether WARP interacts directly with perlecan, intact perlecan isolated from mouse Engelbreth-Holm-Swarm tumor cells was coated onto microtitre plates, and recombinant WARP dimer in solution was added in a standard enzyme-linked immunosorbent assay. WARP bound strongly to immobilized perlecan (1 μg/ml) (see Fig. 6*A*) with an apparent K_D of 23 nM (*inset*). Inclusion of 5 mM $CaCl_2$ or 10 mM EDTA in the incubation and wash buffers did not significantly affect WARP binding to perlecan (not shown).

Perlecan is a modular proteoglycan with a core protein that consists of five distinct domains (Fig. 5*C*). To identify the region within perlecan that interacts with WARP, nine recombinantly expressed perlecan domains (I, I-mut, II, and V) and subdomains (III-1, III-2, III-3, IV-1, and IV-2) (shown in Fig. 5*B*, *lanes 2–10*) were assessed for WARP binding in solid phase assays. In addition to binding to intact perlecan, WARP (50 nM) bound to perlecan domain I and subdomain III-2 but not any other perlecan domains (II and V) or subdomains (III-1, III-3, IV-1, and IV-2) (Fig. 6*B*). Significantly, WARP did not bind to domain I-mut, a mutant variant of domain I that lacks the three heparan sulfate GAG chains (16), suggesting that the interaction with domain I is via the heparan sulfate glycosaminoglycan chains. Saturation binding experiments using WARP over a range of concentrations (0–200 nM) and immobilized domain I, I-mut, and subdomain III-2 confirmed these interactions (Fig. 6*C*). Scatchard analysis derived from five independent binding assays revealed K_D values of 34.0 ± 4.1 for the WARP domain I interaction and 50.6 ± 6.1 for the WARP subdomain III-2 interaction. WARP also bound to heparin, confirming that WARP can associate with heparan sulfate glycosaminoglycan chains (Fig. 6*D*). Because neither the intact perlecan nor any of the recombinant fragments used in the present study were substituted with chondroitin sulfate GAG chains, we cannot test the possibility that WARP interacts with chondroitin sulfate. The heparan sulfate GAG chains substituted on perlecan domain I are ~100 nm in length (20). Quantitation of multiple fields of immunogold electron microscopy images from articular cartilage extracts, comprising more than 200 complexes immunostained for WARP, revealed that 75% of all detected WARP molecules were within 100 nm of perlecan (Fig. 4*D*), consistent with an interaction between WARP and perlecan.

The association between WARP and perlecan was explored further in real time by surface plasmon resonance analysis. WARP was coupled to a CM5 sensor chip, and intact perlecan or recombinant perlecan subdomains were applied to the sensor chip in solution. An interaction was observed with subdomain III-2 but not with intact perlecan or any other subdomains (Fig. 7*A*). Omission of Ca^{2+} or the addition of 10 mM EDTA had no effect on the binding of WARP to fragment III-2 or revealed binding to the other perlecan fragments, indicating that the interaction between WARP and III-2 is not metal ion-dependent, consistent with the analysis of the WARP-perlecan interaction by solid phase assay. The reciprocal binding experiment where subdomain III-2 was coupled to the sensor chip surface and WARP in solution confirmed the interaction (Fig. 7*A*, *inset*). Soluble subdomain III-2 in the concentration range 31–500 nM bound to immobilized WARP dose-dependently (Fig. 7*B*). Consistent with the apparent K_D of 51 nM derived from the solid phase binding assays, global fitting of the WARP domain III-2 interaction data generated a K_D of 44 nM (Langmuir 1:1 binding) with a χ^2 value of 0.96 for the curve fit. The presence of the His tag on WARP allowed assessment of binding of domain III to WARP using ligand capture. In this experiment an anti-His monoclonal antibody was immobilized onto the CM5 sensor chip surface and used to capture His-tagged WARP (Fig. 7*C*). Kinetic analysis demonstrated that domain III-2 bound to captured WARP in a dose-dependent manner (12–400 nM) with a global fit K_D of 34 nM (Langmuir 1:1 binding, $\chi^2 = 0.33$), confirming the high affinity interaction between domain III-2 and WARP.

Although an interaction between WARP-perlecan and WARP domain I was identified in solid phase analysis (Fig. 6*B*), this interaction could not be confirmed in the initial BIAcore studies (Fig. 7*A*). The

reason for the failure to detect an interaction between WARP and domain I or intact perlecan may be related to the carboxymethylated dextran CM5 biosensor surface, which is not recommended for high molecular mass or negatively charged molecules. Perlecan has a 400-kDa core protein and is highly negatively charged because of the GAG chain substitution. To overcome these limitations of the CM5 surface, WARP was coupled to the C1 surface, a more appropriate surface for larger molecules, because it lacks the dextran chains, and the ligand can be coupled directly to the sensor chip surface. We observed dose-dependent binding (25–150 nM) of WARP to perlecan domain I but not mutant domain I that lacks GAG chains, confirming that WARP associates with the heparan sulfate chains of perlecan (Fig. 7*D*). Attempts to fit the curves to a Langmuir 1:1 binding model globally were unsuccessful, suggesting that the interaction between WARP and the heparan sulfate GAG chains is not a straightforward 1:1 interaction. Intact perlecan also bound to WARP coupled to the C1 surface (data not shown).

DISCUSSION

In an effort to understand the role of WARP in cartilage matrix organization, we investigated the tissue forms and distribution of WARP in cartilage and, using recombinantly produced WARP, initiated studies to identify WARP-interacting partners. We report that WARP is specifically localized to the chondrocyte pericellular matrix of articular and fibrocartilages, forms disulfide-bonded multimeric structures, and interacts with the functionally important proteoglycan, perlecan. Our data suggest that WARP forms macromolecular structures that contribute to the assembly and/or maintenance of "permanent" cartilage matrices during development and in mature cartilage.

The distribution of WARP in cartilage is unique. Rather than being widespread throughout the cartilage anlage of the limbs, spine, and sternum that will undergo endochondral ossification, WARP mRNA and protein were restricted to articular cartilage and specialized fibrocartilages. The localization of WARP to the presumptive articular cartilage within the precavitation joint interzone and the absence of matrilin-1 from this tissue provide evidence that articular cartilage is biochemically distinct from epiphyseal cartilage from an early stage rather than persisting as a cartilaginous remnant that fails to undergo differentiation along the endochondral ossification pathway.

In post-natal joints, WARP localizes to the pericellular microenvironment, or chondron, of chondrocytes in articular cartilage and in meniscus. The chondron is a mechanically robust structure that includes the chondrocyte and the surrounding fibrous capsule and is particularly rich in perlecan and type VI collagen, although other ECM components including laminin-1, hyaluronan, fibronectin, and biglycan are also present (reviewed in Ref. 27). The present study identifies WARP as a novel component of this complex macromolecular structure.

WARP shares several similarities with the matrilins including the presence of an N-terminal VWA domain, the ability to form disulfide-bonded multimeric structures in cartilage, and the ability to interact with other cartilage ECM macromolecules (28). Although the guanidine-soluble WARP multimeric structures extracted from cartilage may be composed of WARP bound to other matrix components, similar to the hetero-oligomers formed between matrilin-1 and matrilins-3 (29), -2, and -4 (30), recombinant WARP purified from transfected cells forms oligomers that are reducible to a single 50-kDa monomeric band, suggesting that WARP has the capacity to form large homo-oligomeric structures. The mechanism of WARP multimer assembly remains unclear because WARP does not contain C-terminal heptad repeats similar to the ones found in matrilins (30, 31) or a triple helical domain. Site-directed mutagenesis experiments demonstrated that both cysteine residues participate in intermolecular disulfide bridge formation and that both cysteines are required for stabilization of high molecular mass multimers. The multimerization of WARP potentially brings together a cluster of VWA domains, which might be essential for inter-

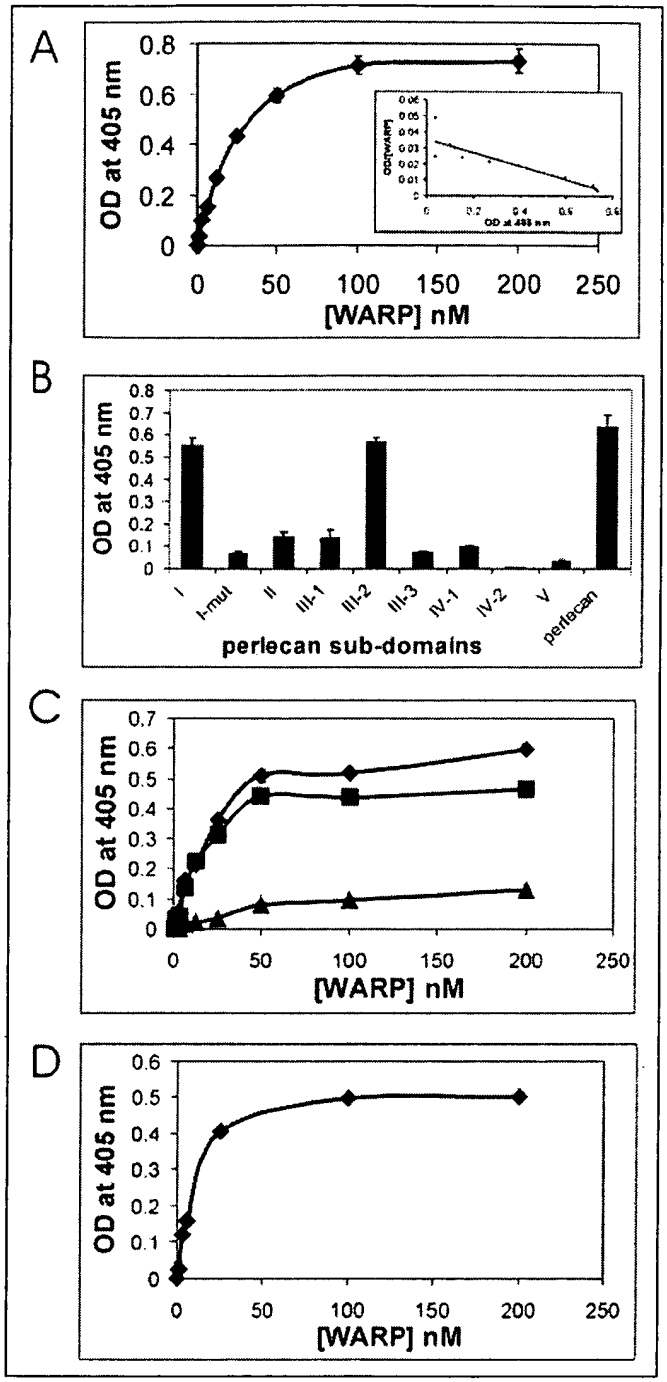

FIGURE 6. **WARP interacts with perlecan in solid phase assays.** *A*, WARP binds to intact perlecan. Perlecan was coated at 1 μg/ml and incubated for 1 h with recombinant WARP (0–200 nM). Bound WARP was detected using polyclonal rabbit anti-C-terminal antiserum, and the data are the means of triplicate determinations ± S.E. *Inset*, Scatchard analysis of binding data reveals an apparent K_D of 23 nM. *B*, WARP interacting with recombinant perlecan fragments. Perlecan domains I, I-mut, II, and V and subdomains III-1, III-2, III-3, IV-1, and IV-2 were coated at 5 μg/ml and incubated for 1 h with recombinant WARP dimer (50 nM). *C*, saturation binding of WARP to perlecan fragments. Perlecan fragment I (diamond), I-mut (*triangle*), and III-2 (square) were plated at 1 μg/ml and incubated with WARP dimer (0–200 nM) in quadruplicate. *D*, binding of WARP to heparin. Heparin was coated at 1 μg/ml and incubated with WARP dimer (0–200 nM).

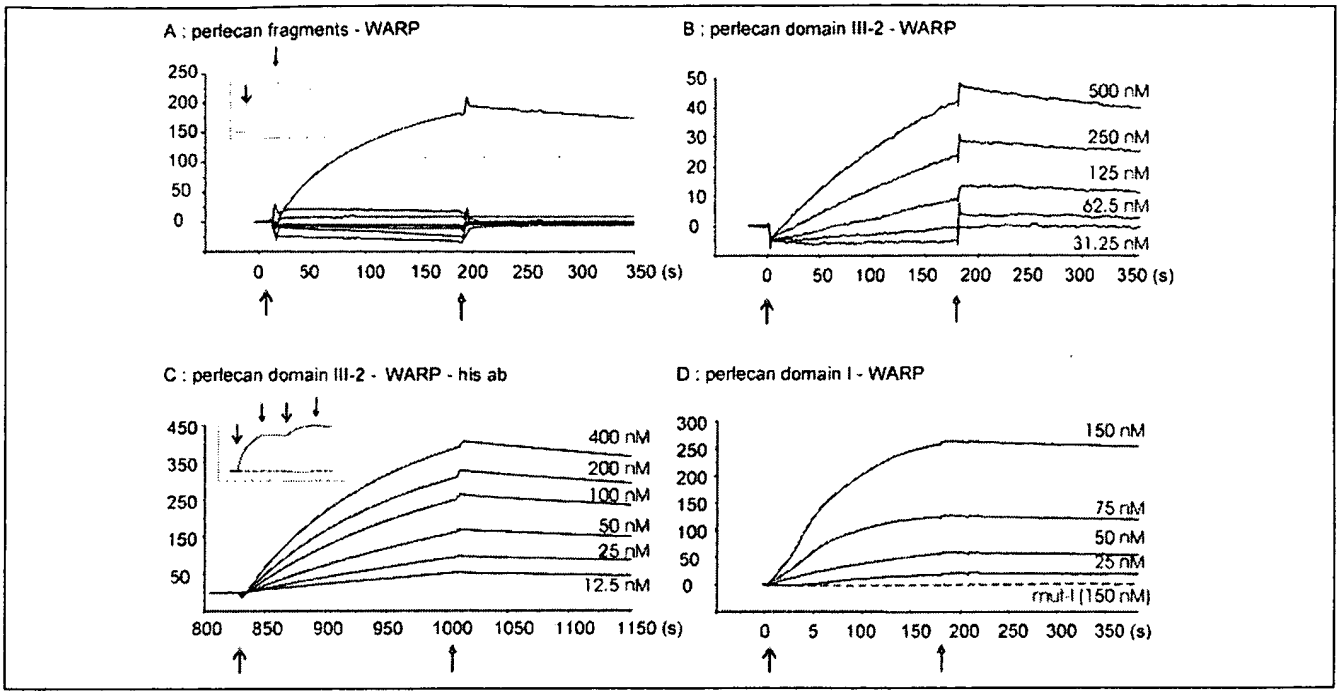

FIGURE 7. **Analysis of WARP-perlecan interaction by surface plasmon resonance.** *A*, WARP binding to perlecan fragments. WARP immobilized on a CM5 sensor chip was presented with intact perlecan and recombinant perlecan fragments I, I-mut, II, III-1, III-2, III-3, IV-1, IV-2, and V in solution in HEPES-buffered saline buffer in the presence of 5 mM $CaCl_2$ injected at a flow rate of 5 μl/min. Domain III-2, but no other perlecan fragments, bound to WARP. *Inset*, reciprocal binding plot showing immobilized domain III-2 interacting with soluble WARP. *B*, kinetic analysis of perlecan subdomain III-2 binding to WARP. Recombinant III-2 (31–500 nM) was injected at 30 μl/min over WARP immobilized to a CM5 surface. Binding of the perlecan fragment is apparent during the association phase followed by the loss of binding during the dissociation phase. Langmuir 1:1 binding curves were fitted globally to the data (K_D = 44 nM) with a χ^2 value for the curve fit of 0.96 (not shown). *C*, analysis of perlecan subdomain III-2-WARP interaction using WARP bound to immobilized anti-His antibody. Recombinant III-2 (12–400 nM) was injected at 30 μl/min over WARP bound to monoclonal His antibody immobilized to CM5 surface. Only the region of the curve showing the association and dissociation of domain III-2 to WARP is shown. Langmuir 1:1 binding curves were fitted globally (R_{max} fitted locally) to the data (K_D = 34 nM) with a χ^2 value for the curve fit of 0.33 (not shown). The *inset* shows a full binding curve including the capture of WARP (first association curve) and subsequent injection of domain III-2 (second association curve). In absence of bound WARP perlecan III-2 did not bind to His antibody (dotted line exhibiting no binding response). *D*, perlecan domain I binding to WARP. Domain I (25–150 nM), injected at 30 μl/min, bound to WARP coupled to C1 sensor surface (*black lines*) in a dose-dependent manner. In contrast, WARP did not bind to mutant domain I (150 nM) lacking heparan sulfate GAG chains (*dotted line* showing no binding to WARP). For all binding curves the data are expressed as the change in relative response units following injection of soluble ligand over sensor chip surface. *Open* and *closed arrows* indicate the start and end of each injection.

actions requiring multiple binding sites, or may function to bring multiple interacting partners into close proximity.

We identified two binding sites for WARP on perlecan: one on subdomain III-2 of the protein core and a second site on the heparan sulfate GAG chains in N-terminal domain I. The perlecan core protein has been shown to associate with a range of basement membrane macromolecules including collagens (IV and XIII), laminin-1, nidogens 1 and 2, β1-integrin, α-dystroglycan, as well as fibulin-2, fibrillin-1, ECM-1, PRELP (proline-arginine-rich end leucine-rich repeat protein), fibronectin, heparin, and several growth factors (platelet-derived growth factor, FGF-2, FGF-7) and FGF-binding protein (19, 32–37).

The cation independence of the interaction between WARP and perlecan suggests that this binding is not mediated by the metal ion-dependent adhesion site motif of the WARP VWA domain. In support of this is the recent finding that the VWA domain of α2 integrin associates with perlecan domain V (38). Our failure to detect WARP binding to domain V argues that the WARP VWA domain is not involved in perlecan interactions, although we cannot exclude an ion-independent interaction with the VWA domain at the present time.

A more likely explanation is that the perlecan-interacting domains of WARP lie within other domains such as the fibronectin type III repeats, because fibronectin has been shown to bind to perlecan or the positively charged C-terminal domain (see below). We are currently conducting further studies to explore these possibilities.

Domain III, the binding site for WARP on the perlecan core protein, has an elongated shape of 30 nm and consists of alternating globular laminin domain IV-like modules separated by rod-like segments composed of laminin-type EGF motifs, an arrangement that is similar to the short arm of laminin α1 chain (18, 39). Although no structural matrix proteins have been reported to interact with domain III, two growth factors have been shown to associate with domain III, FGF-7 and platelet-derived growth factor, which interact with subdomains III-1 and III-2, respectively (34, 40).

We present evidence that WARP interacts with the heparan sulfate GAG chains of perlecan. Several molecules have been shown to form high affinity associations with the heparan sulfate chains of perlecan domain I including collagen IV, fibronectin, the E3 domain of laminin-1 (41), PRELP (33), and the growth factor FGF-2 (42). It has been reported that perlecan isolated from growth plate and articular cartilage contains both chondroitin and heparan sulfate GAG chain substitution (22, 43). Because the perlecan isolated from Engelbreth-Holm-Swarm cells used in our binding studies was only heparan sulfate substituted, we cannot assess whether WARP associates with perlecan substituted with chondroitin sulfate.

PRELP is a cartilage component that belongs to the small leucine-rich repeat protein superfamily and associates with collagen via the LRR domain and the heparan sulfate chains of perlecan domain I via the proline-arginine-rich region (33). WARP has a short proline-arginine-rich sequence at the C terminus, raising the possibility that, as with PRELP, this domain in WARP interacts with the heparan sulfate side chains. An association of positively charged arginine-rich regions with negatively charged GAG chains would be expected to be electrostati-

cally favorable. In addition, because perlecan is known to sequester a range of bioactive compounds such as cytokines and growth factors, WARP binding to the heparan sulfate chains may modify the storage and/or release of these important growth factors. The interaction between WARP and perlecan heparan sulfate chains also suggests that WARP may bind other heparan sulfate proteoglycans such as the cell surface syndecans and glypicans, potentially mediating interactions between chondrocytes and the cartilage ECM. Finally, it has been reported that the GAG-substituted domain I but not the protein backbone is sufficient to initiate the chondrogenic program in pluripotent C3H10T1/2 cells (44). In light of our finding that WARP is present in developing articular cartilage prior to joint formation, one exciting possibility that warrants further investigation is that the WARP perlecan interactions regulate articular cartilage chondrogenesis.

Acknowledgment—We thank Dr. Daniele Belluoccio for providing cartilage extracts.

REFERENCES

1. Boudreau, N., and Bissell, M. J. (1998) *Curr. Opin. Cell. Biol.* **10,** 640–646
2. Hohenester, E., and Engel, J. (2002) *Matrix Biol.* **21,** 115–128
3. Bork, P., Downing, A. K., Kieffer, B., and Campbell, I. D. (1996) *Q. Rev. Biophys.* **29,** 119–167
4. Whittaker, C. A., and Hynes, R. O. (2002) *Mol. Biol. Cell* **13,** 3369–3387
5. Sengle, G., Kobbe, B., Morgelin, M., Paulsson, M., and Wagener, R. (2003) *J. Biol. Chem.* **278,** 50240–50249
6. Veit, G., Kobbe, B., Keene, D. R., Paulsson, M., Koch, M., and Wagener, R. (2006) *J. Biol. Chem.* **281,** 3494–3504
7. Fitzgerald, J., Ting, S. T., and Bateman, J. F. (2002) *FEBS Lett.* **517,** 61–66
8. Fitzgerald, J., and Bateman, J. F. (2003) *FEBS Lett.* **552,** 91–94
9. Chan, D., Weng, Y. M., Hocking, A. M., Golub, S., McQuillan, D. J., and Bateman, J. F. (1996) *J. Biol. Chem.* **271,** 13566–13572
10. Michalczyk, A. A., Allen, J., Blomeley, R. C., and Ackland, M. L. (2002) *Biochem. J.* **364,** 105–113
11. Brown, J. C., Sasaki, T., Gohring, W., Yamada, Y., and Timpl, R. (1997) *Eur. J. Biochem.* **250,** 39–46
12. Kassner, A., Hansen, U., Miosge, N., Reinhardt, D. P., Aigner, T., Bruckner-Tuderman, L., Bruckner, P., and Grassel, S. (2003) *Matrix Biol.* **22,** 131–143
13. Braissant, O., and Wahli, W. (1998) *Biochemica* **1,** 10–16
14. Goldoni, S., Owens, R. T., McQuillan, D. J., Shriver, Z., Sasisekharan, R., Birk, D. E., Campbell, S., and Iozzo, R. V. (2004) *J. Biol. Chem.* **279,** 6606–6612
15. Costell, M., Mann, K., Yamada, Y., and Timpl, R. (1997) *Eur. J. Biochem.* **243,** 115–121
16. Sasaki, T., Costell, M., Mann, K., and Timpl, R. (1998) *FEBS Lett.* **435,** 169–172
17. Costell, M., Sasaki, T., Mann, K., Yamada, Y., and Timpl, R. (1996) *FEBS Lett.* **396,** 127–131
18. Schulze, B., Mann, K., Battistutta, R., Wiedemann, H., and Timpl, R. (1995) *Eur. J. Biochem.* **231,** 551–556
19. Hopf, M., Gohring, W., Kohfeldt, E., Yamada, Y., and Timpl, R. (1999) *Eur. J. Biochem.* **259,** 917–925
20. Paulsson, M., Yurchenco, P. D., Ruben, G. C., Engel, J., and Timpl, R. (1987) *J. Mol. Biol.* **197,** 297–313
21. Hauser, N., Paulsson, M., Heinegard, D., and Morgelin, M. (1996) *J. Biol. Chem.* **271,** 32247–32252
22. SundarRaj, N., Fite, D., Ledbetter, S., Chakravarti, S., and Hassell, J. R. (1995) *Journal of Cell Science* **108,** 2663–2672
23. Melrose, J., Smith, S., Ghosh, P., and Whitelock, J. (2003) *J. Histochem. Cytochem.* **51,** 1331–1341
24. Iozzo, R. V., Cohen, I. R., Grassel, S., and Murdoch, A. D. (1994) *Biochem. J.* **302,** 625–639
25. Timpl, R. (1993) *Experientia* **49,** 417–428
26. Costell, M., Gustafsson, E., Aszodi, A., Morgelin, M., Bloch, W., Hunziker, E., Addicks, K., Timpl, R., and Fassler, R. (1999) *J. Cell Biol.* **147,** 1109–1122
27. Poole, C. A. (1997) *J. Anat.* **191,** 1–13
28. Wiberg, C., Klatt, A. R., Wagener, R., Paulsson, M., Bateman, J. F., Heinegard, D., and Morgelin, M. (2003) *J. Biol. Chem.* **278,** 37698–37704
29. Wu, J. J., and Eyre, D. R. (1998) *J. Biol. Chem.* **273,** 17433–17438
30. Frank, S., Schulthess, T., Landwehr, R., Lustig, A., Mini, T., Jeno, P., Engel, J., and Kammerer, R. A. (2002) *J. Biol. Chem.* **277,** 19071–19079
31. Haudenschild, D. R., Tondravi, M. M., Hofer, U., Chen, Q., and Goetinck, P. F. (1995) *J. Biol. Chem.* **270,** 23150–23154
32. Mongiat, M., Otto, J., Oldershaw, R., Ferrer, F., Sato, J. D., and Iozzo, R. V. (2001) *J. Biol. Chem.* **276,** 10263–10271
33. Bengtsson, E., Morgelin, M., Sasaki, T., Timpl, R., Heinegard, D., and Aspberg, A. (2002) *J. Biol. Chem.* **277,** 15061–15068
34. Mongiat, M., Taylor, K., Otto, J., Aho, S., Uitto, J., Whitelock, J. M., and Iozzo, R. V. (2000) *J. Biol. Chem.* **275,** 7095–7100
35. Tiedemann, K., Sasaki, T., Gustafsson, E., Gohring, W., Batge, B., Notbohm, H., Timpl, R., Wedel, T., Schlotzer-Schrehardt, U., and Reinhardt, D. P. (2005) *J. Biol. Chem.* **280,** 11404–11412
36. Mongiat, M., Fu, J., Oldershaw, R., Greenhalgh, R., Gown, A. M., and Iozzo, R. V. (2003) *J. Biol. Chem.* **278,** 17491–17499
37. Tu, H., Sasaki, T., Snellman, A., Gohring, W., Pirila, P., Timpl, R., and Pihlajaniemi, T. (2002) *J. Biol. Chem.* **277,** 23092–23099
38. Bix, G., Fu, J., Gonzalez, E. M., Macro, L., Barker, A., Campbell, S., Zutter, M. M., Santoro, S. A., Kim, J. K., Hook, M., Reed, C. C., and Iozzo, R. V. (2004) *J. Cell Biol.* **166,** 97–109
39. Murdoch, A. D., Dodge, G. R., Cohen, I., Tuan, R. S., and Iozzo, R. V. (1992) *J. Biol. Chem.* **267,** 8544–8557
40. Gohring, W., Sasaki, T., Heldin, C. H., and Timpl, R. (1998) *Eur. J. Biochem.* **255,** 60–66
41. Battaglia, C., Mayer, U., Aumailley, M., and Timpl, R. (1992) *Eur. J. Biochem.* **208,** 359–366
42. Whitelock, J. M., Murdoch, A. D., Iozzo, R. V., and Underwood, P. A. (1996) *J. Biol. Chem.* **271,** 10079–10086
43. Govindraj, P., West, L., Koob, T. J., Neame, P., Doege, K., and Hassell, J. R. (2002) *J. Biol. Chem.* **277,** 19461–19469
44. French, M. M., Gomes, R. R., Jr., Timpl, R., Hook, M., Czymmek, K., Farach-Carson, M. C., and Carson, D. D. (2002) *J. Bone Miner. Res.* **17,** 48–55